Joint Pathology Center
Veterinary Pathology Services

WEDNESDAY SLIDE CONFERENCE 2024-2025

Conference #9 — 16 October 2024

CASE I:

Signalment:
7-year-old female black and white colobus monkey (*Colobus guereza*).

History:
The animal was housed at a UK zoo collection as part of a colobus/patas monkey exhibit. It presented subdued and with reduced appetite; after a short period of clinical improvement the animal was found unable to move and was euthanized based on a poor prognosis. Previous appropriate fecal testing at a specialized laboratory was repeatedly positive for *Entamoeba species* for a period of 8 months prior to death. A male in the same group had also died in the past 5 months.

Gross Pathology:
The animal presented in poor body condition with no subcutaneous fat and widespread serous fat atrophy. Approximately 750ml of orange-yellow fluid were present in the abdominal cavity. The glandular portion of the stomach had a circular, 2cm diameter, slightly depressed, ulcer with a thin white and red halo (hyperemia). The liver showed a focal capsular adhesion to the gastric serosa. Cut surfaces displayed a diffusely enhanced lobular pattern and exhibited multifocal, dark yellow, 5mm to 5cm, nodular foci randomly distributed throughout the parenchyma. The right cranial lung lobe exhibited a focal, 4cm, mottled yellow-white and red nodule, with heterogeneously necrotic and mucopurulent

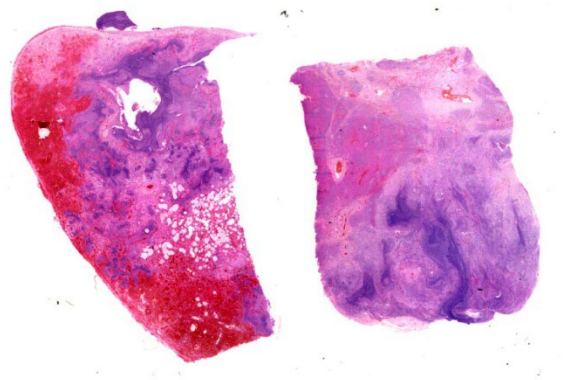

Figure 1-1. Lung and liver, colobus monkey. Much, if not all, of the subgross architecture of the sections of lung (left) and liver (right) is effaced by extensive areas of necrosis, hemorrhage, and abundant, often lamellated cellular debris. (HE, 4X)

cut surfaces. The middle right lung lobe was mottled red to dark-red and firm (consolidated). The left lung lobe had patchy areas of congestion. Remaining organs and body cavities were unremarkable on macroscopic examination.

Laboratory Results:
Clinical Pathology:

Liver, impression smear: Accumulations of degenerate neutrophils and vacuolated macrophages, including large central aggregations of densely cellular basophilic necrotic debris. Red blood cells and occasional multinucleated cells were present around the periphery of aggregates. A few normal hepatocytes were seen, with blue cytoplasm containing occasional dark blue/black granules

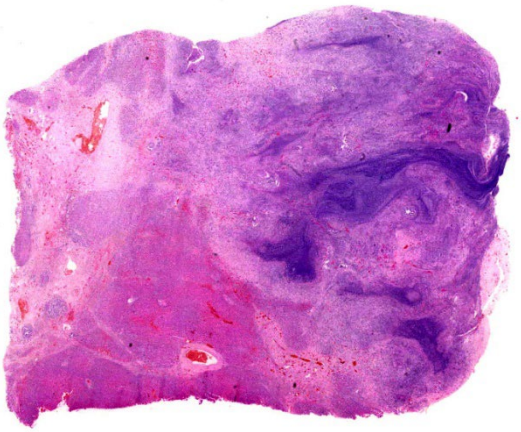

Figure 1-2. Liver, colobus monkey. 50% of the liver is effaced by large areas of necrosis. At the periphery of the necrosis, there is prominent fibrosis throughout the remainder of the section. (HE, 7X)

(presumed hemosiderin). Mixed populations of bacteria were present amongst the cellular debris. Some areas had more abundant populations of spindle cells (presumptive fibroblasts).

Right lung, impression smear: Mixed populations of inflammatory cells including small numbers of degenerate neutrophils, abundant macrophages, and occasional multinucleated cells. Macrophages had vacuolated cytoplasm, sometimes with intracytoplasmic granular debris. Red blood cells were intermingled with inflammatory populations.

Immunohistochemistry:

IHC for *E. histolytica*: Positive (carried out at the Institute for Veterinary Pathology, University of Liverpool, following standard operating procedures).

Microscopic Description:

Liver: Randomly to bridging, approximately 80% of the examined section is completely effaced by multifocal to coalescent areas containing abundant amphophilic and basophilic amorphous debris (lytic necrosis) admixed with cytoclastic inflammatory cells, small numbers of viable and non-viable neutrophils, and moderate numbers of circular to oval, 15-20µm, unicellular protozoa with a pale eosinophilic cytoplasm with large phagocytic vacuoles and a pale small amphophilic eccentric basophilic round to oval nucleus (amoebic trophozoites). Areas of necrosis are intermingled and rimmed by numerous macrophages, neutrophils (viable and non-viable) and occasional multinucleated giant cells (Foreign body giant cell type) admixed with moderate deposition of reactive fibroblasts and mature collagen fibers (fibrosis). Interlacing and incorporating between the immature granulation and fibrotic tissue, there are myriad of irregular proliferated biliary ductules (biliary hyperplasia or ductular reaction). The adjacent parenchyma is composed of widely separated hepatic cords with small, irregular hepatocytes (atrophy).

Lung: Multifocal to coalescing, affecting approximately 75% of the section, there is severe pyogranulomatous and necrotizing inflammation accompanied by large empty ar-

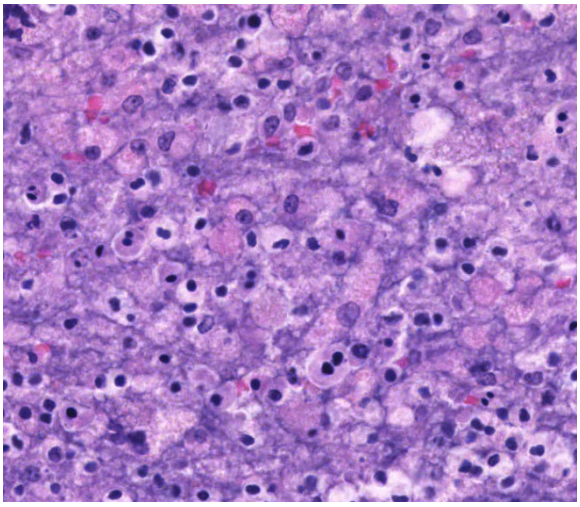

Figure 1-3. Liver, colobus monkey. There are numerous amebae within the areas of lytic necrosis. Amebae are round with prominent nuclei and abundant eosinophilic granular cytoplasm. (HE, 567X).

eas (cavitation of alveolar parenchyma) and dilated bronchi (bronchiectasis). Filling and expanding bronchi and bronchioles and effacing the adjacent pulmonary parenchyma, there are large numbers of amphophilic karyorrhectic and cellular debris (lytic necrosis), eosinophilic fibrillary beaded material (fibrin), viable and degenerated neutrophils, macrophages and extravasated erythrocytes (hemorrhage) admixed with orange/yellow hemoglobin breakdown pigments. Within the necrotic areas there are numerous circular or oval, 15-20µm, unicellular protozoa with a pale eosinophilic cytoplasm with large phagocytic vacuoles and pale small amphophilic eccentric round to oval nucleus (amoebic trophozoites). The necrotic areas are surrounded by abundant viable and degenerate neutrophils, macrophages (mostly epithelioid) and multinucleated giant cells (Langhans and foreign body type). Focally, there is a large thrombus filling a pulmonary vessel which is attached to the necrotic endothelium and composed of neutrophils, necrotic debris and fibrin. Multifocally, surrounding areas of inflammation, alveolar septa are expanded or effaced by increased collagen (fibrosis) and hypertrophic fibroblasts with perpendicularly arranged small blood vessels (granulation tissue). Adjacent septa are irregularly lined by cuboidal epithelium (pneumocyte type II hyperplasia). Less affected alveolar spaces are filled with a large amount of hemorrhage, occasionally admixed with fibrin, inflammatory debris and necrotic material. Multifocally, there are few discrete areas of pulmonary over inflation.

Contributor's Morphologic Diagnosis:
1. Hepatitis, necrotizing, pyogranulomatous, fibrosing, with abundant intralesional protozoal (amoebic) trophozoites consistent with *Entamoeba* spp., and bile duct hyperplasia, severe, multifocal to coalescent, random to bridging), chronic-active; liver.

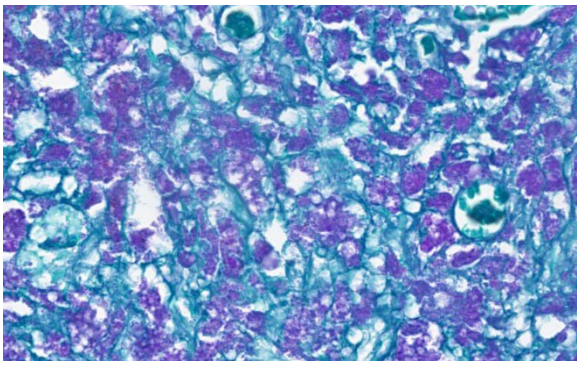

Figure 1-4. Liver, colobus monkey. A PAS stain demonstrates the amebae within areas of lytic necrosis. (PAS w/ malachite green, 200X)

2. Pneumonia, necrotizing, pyogranulomatous, with bronchiectasis, fibrin thrombus, and intralesional protozoal (amoebic) trophozoites consistent with *Entamoeba* spp., severe, multifocal to coalescent, chronic-active; lung.

Contributor's Comment:
Lesions in this case were consistent with chronic-active hepatic and pulmonary amebiasis. Other concomitant lesions in this case included ulcerative amebic gastritis, ascites, and emaciation. Unicellular protozoal organisms whose morphology were consistent with *Entamoeba* spp. were observed within the necrotic areas in the liver, lung, and stomach. Immunohistochemistry for *Entamoeba histolytica* was positive, further confirming the histopathological diagnosis.

E. histolytica is a protozoan parasite reported worldwide to occur in humans and a wide range of New and Old World monkeys, as well as apes.[8] Several species have been described which differ in their location in the host and nonhuman primate (NHP) species affected including *E. histolytica, E. dispar, E. moshkovskii, E. polecki, E. nutalli, E. chattoni, E. coli, E. hartmanni, E. ecuadoriensis and E. bangladeshi*.[8] In the United Kingdom, one study suggests a notable prevalence of

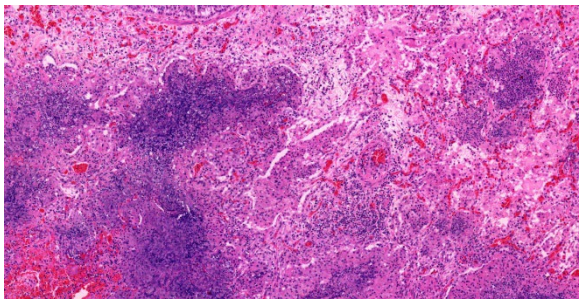

Figure 1-5. Lung, colobus monkey. There are numerous areas of lytic necrosis and alveolar exudate throughout the lung. (HE, 87X)

Entamoeba infection in NHPs with three main species circulating in the zoo's environment, namely *E. histolytica*, *E. dispar* and *E. polecki* ST4.[6]

Included under the *E. histolytica* species complex are *E. histolytica, E. dispar* and *E. moshkovskii.* They have different virulence capabilities, but are morphologically indistinguishable.[7] *E. histolytica* is the most commonly recognized zoonotic agent and can cause both intra- and extraintestinal disease.[1,8] There is a zoonotic risk for humans in close contact with primates.[6] The pathogenicity is determined by multiple virulence factors such as ubiquitin and adhesive surface lectins and is further depend on strain, host species, nutritional status, gastrointestinal (GI) microflora, environmental factors.[1,2,8] The essential steps leading to tissue damage are the adhesion of the organism to the hosts' protective mucus by lectin followed by enzymatic mucus breakdown and lectin-mediated adherence to host epithelium. Damage to mucosal epithelium is mediated by the release of cysteine proteases that attract inflammatory cells.

Usually, clinical signs are unspecific and NHPs show lethargy, weakness apathy, dehydration, anorexia, vomiting, rectal prolapse and severe catarrhal or hemorrhagic diarrhea.[1,8]

Fatal amebiasis with abscess formation particularly in the liver and more infrequently in the lung and the brain is reported in humans, colobus monkeys (*Colobus guereza*; *Colobus abyssinicus*), douc langurs (*Pygathrix nemaeus*), dusky leaf monkeys (*Presbytis obscurus*), chimpanzees (*Pan troglodytes*), baboons (*Papio* spp.), orangutans (*Pongo pygmaeus*), and spider monkeys (*Ateles* spp.).[1,6,8,9] Concurrent amebic gastritis is predominantly seen in leaf-eating primates (colobus monkey, silver-leafed monkey) and other gastric fermenting folivores such as langurs and proboscis and relates to higher stomach pH that is conducive to survival of ameba.[1,9]

The encystment of the infective forms appears to take place in the small intestine and the infection is established in the lumen of the large intestine. Infections are often transient and self-limiting. Under certain circumstances however, *E. histolytica* may invade the intestinal wall and cause colitis and consecutive amebic hepatitis by spread via the portal vein.[9] Hematogenous and/or lymphatic invasion of other organs (brain, lung) is rare and reported to be nearly always associated with liver abscesses.[8]

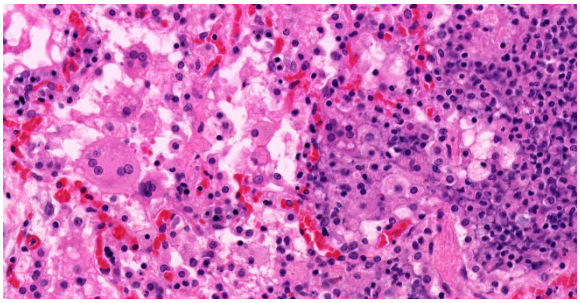

Figure 1-6. Lung, colobus monkey. Ameba are present within areas of necrosis. There are scattered multinucleated foreign body type giant cells within the alveoli as well. (HE, 443X)

Microscopically, amebae are surrounded by a clear halo with extensive pseudopodia and possess a nucleus with a dark karyosome. The cytoplasm appears foamy and they frequently phagocytize erythrocytes, which makes them difficult to distinguish from activated macrophages. The periodic acid-Schiff reaction highlights intracytoplasmic glycogen granules within amebae. Trichrome and Giemsa stains can also be utilized to emphasize amoebic trophozoites. On direct smears, Lugol's iodine can be used to aid the diagnosis of trophozoites, due to the presence of intracytoplasmic glycogen (starch).

Contributing Institution:
International Zoo Veterinary Group, Station House, Parkwood Street, Keighley, BD21 4NQ, UK. Website: www.izvg.co.uk

JPC Diagnosis:
1. Liver: Hepatitis, necrotizing, chronic-active, multifocal to coalescing, severe, with numerous amebic trophozoites.
2. Lung: Pneumonia, interstitial, necro-hemorrhagic, chronic-active, diffuse, severe, with pleural granulation tissue and numerous amebic trophozoites.

JPC Comment:
This week's moderator was Dr. Jeremy Bearss, previous chairman of the department and current research pathologist with the National Institute of Allergy and Infectious Diseases. This week's cases were chosen as they are all excellent "descriptive cases".

The profoundly necrotizing nature of these lesions was evident from low magnification, although more careful observation was required to pick up evidence of chronicity including type II pneumocyte hyperplasia, fibrosis, and subpleural granulation tissue within the lung and nodular regeneration and biliary hyperplasia within the liver. Although amebae were recognizable in large numbers

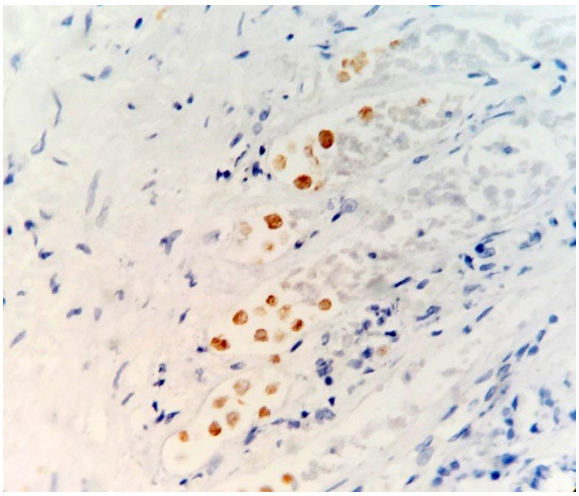

Figure 1-7. Stomach, colobus monkey. Ameba within the gastric ulcer are positive for an immunostain for *Entamoeba histolytica*. (anti *Entamoeba histolytica*, 400X) (*Photo courtesy of*: International Zoo Veterinary Group, Station House, Parkwood Street, Keighley, BD21 4NQ, UK. Website: www.izvg.co.uk)

on H&E, both PAS and GMS stains were helpful in highlighting them, and are consoiderations for cases in whichch their numbers are reduced.

As the contributor notes, diet plays a role in the pathogenesis of this entity in leaf-eating primates. Colobine monkeys have a large simple stomach with four compartments, which provide dedicated space for increased fermentation.[3] The relative increase in pH in this portion of the stomach is conducive to the survival of ameba. The gastric ulcers noted in the clinical history are the portal of entry of *Entamoeba* into the portal system with dissemination to liver and lungs. Dr. Kali Holder (Smithsonian conservation pathologist) was among conference attendees and noted that similar *Entamoeba* lesions can be seen in kangaroos and wallabies given their similar diet and compartmented stomach structure.

Finally, the role of *Entamoeba* as both a zo-

onosis and anthrozoonosis is worth considering. Transmission of *Entamoeba* from captive non-human primates to caretakers was previously described.[5] *E. nuttalli* is pathogenic in animals, though its role in human disease is unclear. Nonetheless, caretakers that did not care for NHPs lacked the presence of *E. nuttalli* in fecal specimens, consistent with transmission of the agent within the zoo environment. Conversely, potential transmission of *E. histolytica* from humans to chimpanzees and baboons in the Gombe region of Tanzania has also been detailed.[4]

References:

1. Calle P, Joslin J. Chapter 37 - New World and Old World monkeys. In: Miller R, Fowler M, eds. *Fowler's Zoo and Wild Animal Medicine, Volume 8*. St. Louis, Missouri: Elsevier Inc.; 2015:301–335.
2. Crisóstomo-Vázquez MDP, Jiménez-Cardoso E, Arroyave-Hernández C. Entamoeba histolytica sequences and their relationship with experimental liver abscesses in hamsters. *Parasitol Res*. 2006;98:94–98.
3. Davies G, Oates J. *Colobine Monkeys: Their Ecology, Behaviour and Evolution*. New York, Cambridge University Press, 1994, pp. 205-284.
4. Deere JR, Parsons MB, Lonsdorf EV, et al. Entamoeba histolytica infection in humans, chimpanzees and baboons in the Greater Gombe Ecosystem, Tanzania. *Parasitology*. 2019;146(9):1116-1122.
5. Levecke B, Dorny P, Vercammen F, et al. Transmission of Entamoeba nuttalli and Trichuris trichiura from Nonhuman Primates to Humans. *Emerging Infectious Diseases*. 2015;21(10):1871-1872.
6. Regan CS, Yon L, Hossain M, Elsheikha HM. Prevalence of Entamoeba species in captive primates in zoological gardens in the UK. *PeerJ*. 2014;DOI 10.7717/peerj.492.
7. Sargeaunt P, Williams JE, Jones DM. Electrophoretic Isoenzyme Patterns of Entamoeba histolytica and Entamoeba chattoni in a Primate Survey. *J Protozool*. 1982;29:136–139.
8. Strait K, Else J, Eberhard M. Parasitic diseases of nonhuman primates. In: Abee CR, Mansfield K, Tardif S, Morris T, eds. *Nonhuman Primates in Biomedical Research: Diseases, Vol.2*. London: Elsevier Inc.; 2012:197–297.
9. Ulrich R, Böer M, Herder V, et al. Epizootic fatal amebiasis in an outdoor group of Old World monkeys. *J Med Primatol*. 2010;39:160–165.

CASE II:

Signalment:
13 year old, castrated male, Yorkshire terrier, *Canis familiaris*, Dog

History:
History of inflammatory bowel disease treated with prednisone. Presented on 17 January 2024 for evaluation of dyspnea and hyporexia. Had multiple episodes of vomiting without response to an increased prednisone dose. He was hospitalized on supplemental O2. Exam revealed a grade 4/6 heart

Figure 2-1. Lung, dog. Two sections of lung are submitted for examination. There are several foci of hypercellularity in subpleural areas.. (HE, 5X)

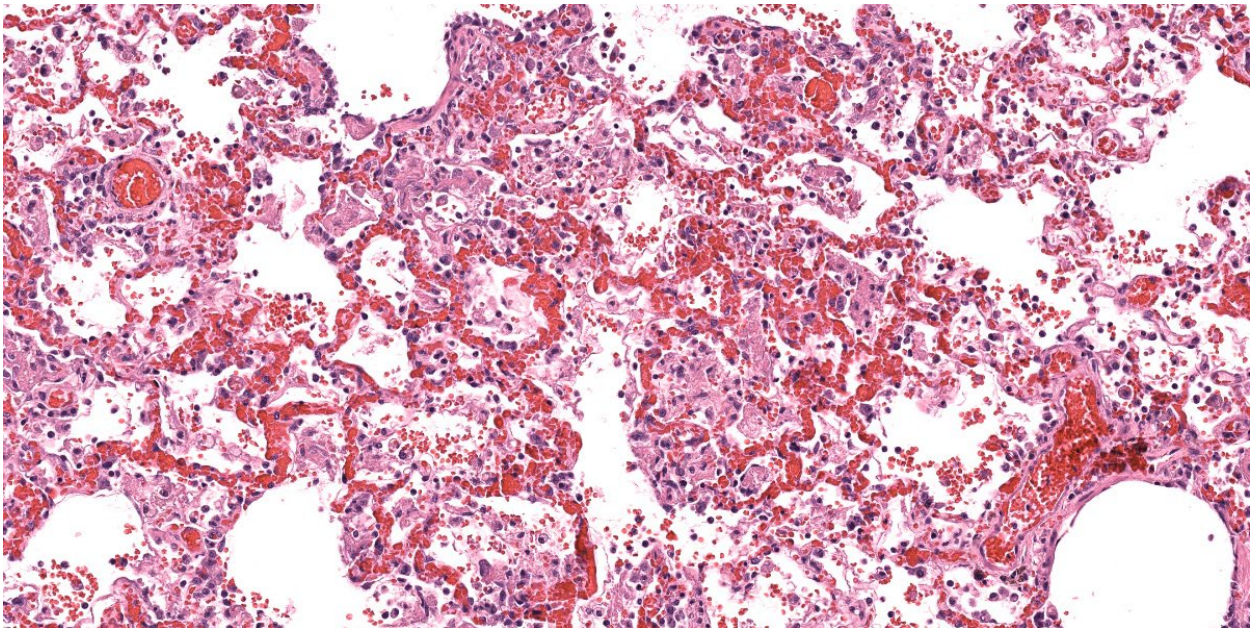

Figure 2-2. Lung, dog. in one section, in a patchy distribution, there are extensive areas in which alveolar septa are congested with intraseptal edema. There is exudation of fibrin into the alveoli, where it has polymerized and is admixed with hemorrhage, alveolar macrophages and neutrophils. (HE, 381X)

murmur, he was preemptively treated with Vetmedin/Lasix. Radiographs showed evidence of pneumonia. Echocardiogram revealed evidence of mitral and tricuspid valve degeneration with regurgitation, with no left atrial enlargement and no evidence of congestive heart failure. Patient was transitioned to room air on 18 January 2024 and he did well. On the morning of 19 January 2024, patient acutely decompensated and CPR was performed. CPR was successful but patient was euthanized.

Gross Pathology:
Heavy body condition, BCS 7/9, and distended abdomen. Lungs were diffusely wet and heavy, red fluid in the thoracic cavity. The right ventricle was large and dilated, and there were nodular proliferations on the right and left AV valves. No significant findings in the abdominal cavity.

Microscopic Description:
Lungs: Alveolar septa are diffusely thickened by variable combinations and concentrations of fibrin, histiocytes, fewer lymphocytes, edema, and congested alveolar capillaries. Multifocally affecting approximately 40% of the examined tissue, alveolar septa are lined by lamellae of polymerized eosinophilic hyaline material (hyaline membranes), and in these areas type I pneumocytes are often lost or necrotic with nuclear pyknosis or karyorrhexis. Diffusely, alveolar spaces contain variable combinations and concentrations of hemorrhage, edema fluid, variably polymerized fibrin, and increased numbers of foamy alveolar macrophages that occasionally contain phagocytosed erythrocytes and rarely contain hints of cytoplasmic hemosiderin. The perivascular tissue surrounding larger vessels is expanded by edema. The adventitia of small and medium veins multifocally is minimally to mildly expanded by increased fibrous connective tissue. Focally extensively affecting approximately 5% of the examined

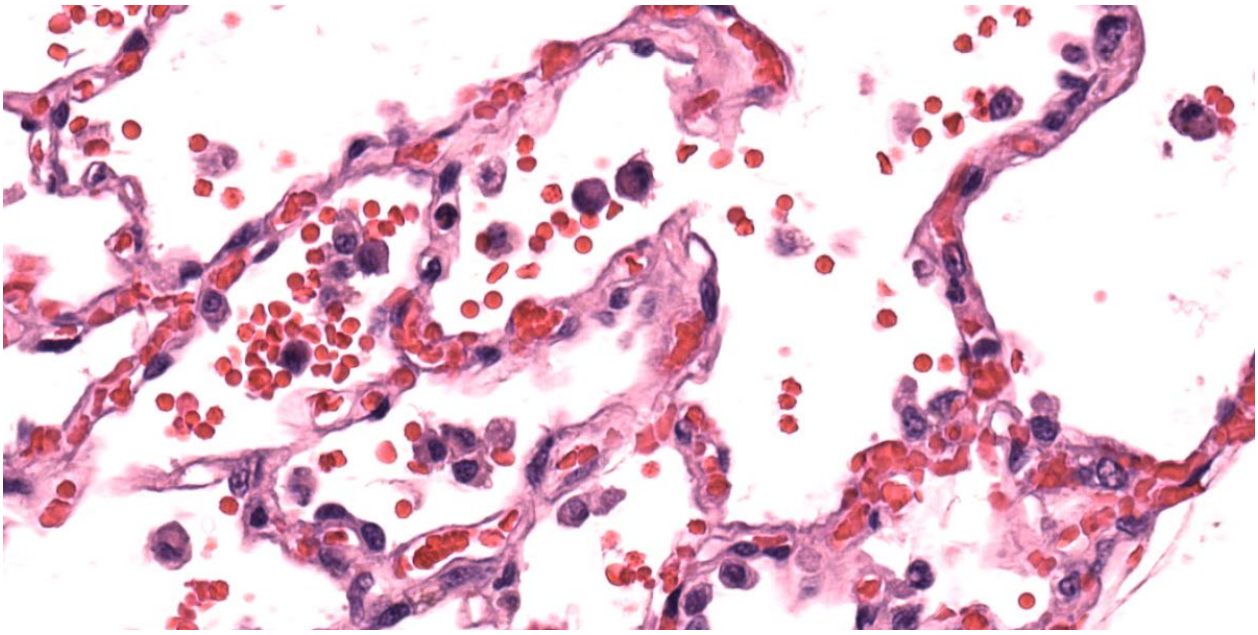

Figure 2-3. Lung, dog. Throughout the section, alveolar spaces contain clusters of macrophages which contain intracytoplasmic brown granular pigment (iron), know as "heart failure cells". (HE, 248X)

tissue, adjacent to a bronchus and pulmonary vein, alveoli are filled and expanded by extracellular and intrahistiocytic amorphous, homogeneous, amphophilic, anisotropic, aggregates of hyaline material that vary in size from 5-300 in diameter. The material is multifocally surrounded by granulomatous inflammation composed of foamy macrophages, multinucleate giant cells, and few lymphocytes and plasma cells. At the tip of the margin of one tissue section, there is a focal area of moderate to marked alveolar septal expansion by fibrosis. In this area, there is marked type II pneumocyte hyperplasia, and alveoli contain high numbers of entrapped foamy alveolar macrophages.

The intra-alveolar, hyaline, amphophilic material is strongly PAS-positive.

Not submitted for WSC, the liver had evidence of chronic passive congestion to include central vein adventitial fibrosis, centrilobular congestion, and centrilobular hepatocyte atrophy.

Contributor's Morphologic Diagnosis:

1. Lung: Pneumonia, interstitial, acute, necrotizing, multifocal to coalescing, moderate, with hyaline membrane formation
2. Lung: Congestion, diffuse, moderate, with increased alveolar macrophages and perivascular edema
3. Lung: Pneumonia, granulomatous, focal, mild, with intraalveolar, extracellular and intrahistiocytic, amphophilic, homogeneous, hyaline material

Contributor's Comment:

This case represents three pulmonary entities: acute respiratory distress syndrome, chronic passive congestion, and pulmonary hyalinosis.

Acute respiratory distress syndrome (ARDS) is the clinical manifestation of diffuse alveolar damage (DAD).[4,5,7] DAD is due to injury to type I pneumocytes and/or alveolar capillary endothelium which results in serum leakage into alveoli, with subsequent pulmonary edema and polymerization of fibrin into characteristic hyaline membranes lining alveolar

septa, and eventually type II pneumocyte hyperplasia and interstitial fibrosis.[5,7] The pathophysiology of ARDS/DAD is beautifully illustrated in *Robbins and Cotran Pathologic Basis of Disease* 10th Ed. Figure 15.3.[5] ARDS has garnered widespread attention in recent years because the pathogenesis of COVID-19-induced pneumonia is similar.[7] Clinically, animals affected with ARDS have acute-onset dyspnea, tachypnea, variable coughing, and lethargy that is often fatal within 3 days.[4] The key histologic feature of this condition is the formation of hyaline membranes; these are variably thick, eosinophilic membranes lining alveolar septa, which physiologically prevent gas diffusion leading to respiratory distress.[4] Histologically there is also often necrosis or attenuation of terminal bronchiolar epithelium.[4,7] DAD may be due to direct or indirect damage, such as the result of multiple organ dysfunction syndrome.[4,7] Notable causes of diffuse alveolar damage include smoke inhalation, oxygen toxicity, inhalation of toxic gases (ammonia, phosgene, ozone, etc.), toxin ingestion (paraquat, 3-methylindole, perilla mint, etc.), near drowning, strangulation, septicemia, shock, massive trauma, and chronic left sided heart failure, although many cases are idiopathic.[4,5,7]

In humans, congestive left-sided heart failure with subsequent pulmonary congestion often results in accumulation of so-called "heart failure cells" within alveoli.[6] These "heart failure cells", also termed siderophages, are simply hemosiderin-laden alveolar macrophages that have phagocytosed red blood cells.[4,6,7] In veterinary medicine (with the exception of non-human primates), it is rare to see classic "heart failure cells" associated with chronic heart failure; however, the number of non-hemosiderin-laden alveolar macrophages is often increased secondary to chronic pulmonary edema.[4] Additionally of note, hemosiderin-laden alveolar macrophages can be present in conditions other

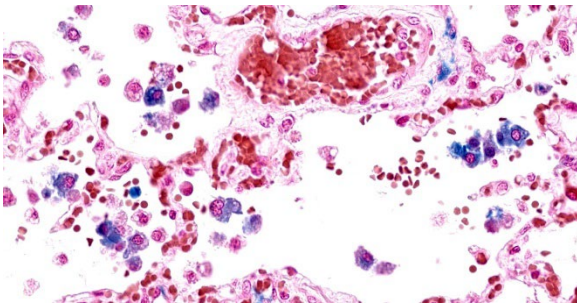

Figure 2-4. Lung, dog. A Perl's stain for iron demonstrates numerous iron pigment in the "heart failure cells". (Perl's iron, 400X)

than heart failure, such as pulmonary hemorrhage.[4] Pulmonary sequelae to chronic left-sided heart failure are pulmonary edema, increased alveolar macrophages, and pulmonary vein remodeling.[4,7] The pulmonary vein remodeling may simply consist of subtly increased adventitial collagen of small to medium-sized pulmonary veins.[4]

Pulmonary hyalinosis is an uncommon, idiopathic condition in older dogs that is due to an uncharacterized alveolar-filling disorder.[7,8] Alveolar-filling disorders are characterized by accumulations of abnormal material in alveoli, and include alveolar histiocytosis, endogenous lipid pneumonia, alveolar proteinosis, alveolar phospholipidosis, alveolar microlithiasis, and pulmonary hyalinosis.[7,8] Pulmonary hyalinosis is considered an incidental finding.[4,7,8] The material within alveolar lumina is characteristically amphophilic, amorphous or lamellar, birefringent, and strongly PAS-positive.[4,7,8] This condition was relatively recently reported in 6 captive sugar gliders.[8] This condition was also recently highlighted in the JPC Wednesday Slide Conference (see Conference 5, Case 4, 2022-2023).

Contributing Institution:
Tri-Service Research Laboratory

4141 Petroleum Dr

San Antonio, TX 78234

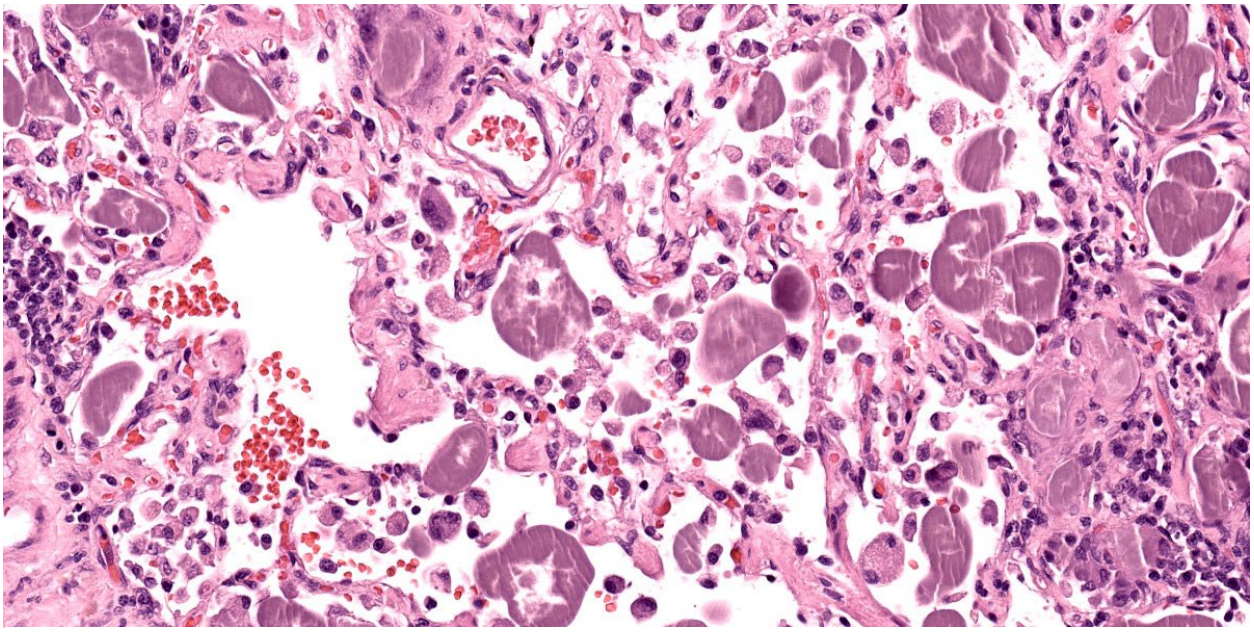

Figure 2-5. Lung, dog. Multifocally, there are foci of pulmonary hyalinosis with abundant amphophilic protein within alveoli. (HE, 390X)

JPC Diagnosis:

1. Lung: Pneumonia, interstitial and organizing, necrotizing and fibrinous, subacute, multifocal, moderate with type II pneumocyte hyperplasia.
2. Lung: Congestion, chronic, diffuse, mild to moderate with alveolar siderophages and edema.
3. Lung: Pneumonia, interstitial, granulomatous, chronic, multifocal, moderate, with abundant hyaline material.
4. Lung: Pneumonitis, lymphocytic, chronic, focal, marked (subpleural alveolar proteinosis).

JPC Comment:

Case 2 showcases multiple entities occurring simultaneously in the lung of an aged dog. Conference participants collectively were able to spot five distinct processes, which reinforces the value of complete slide examination. We did not add a morphologic diagnosis for anthracosilicosis in this case, as it is a common and incidental finding in aged animals, and of a relatively minor degree in this case. Likewise, the pulmonary hyalinosis in this case was not likely significant in the death of this animal. We added a separate morphologic diagnosis for the subpleural alveolar proteinosis, which is a common incidental finding in older dogs, but is worth noting.

The group differed from the contributor in their interpretation of hyaline membranes in this case. Participants noted that the polymerized fibrin filled the alveoli as "fibrin ball"[1,3] as opposed to a hyaline membrane, which is typically adherent to the basement membrane itself and visually lines the affected septa.. Likewise, the concurrent type II pneumocyte hyperplasia in this case and increased number of myofibroblasts highlighted by a smooth muscle actin IHC was consistent with at least a subacute course of disease in this animal. Dr Bearss noted that he has seen this phenotype in monkeys utilized for Nipah virus research and drew parallels from his experience

Acute fibrinous and organizing pneumonias

(AFOP) are a distinct entity in human medicine[1,2,3] that represent an acute to subacute phenotype of severe lung injury. With this slower onset, the mix of plasma protein, surfactant, fibrin, and cellular debris characteristic of a classic acute hyaline membrane is infiltrated by inflammatory cells and embedded myofibroblasts and forms a distinct "fibrin ball" in the alveolus. Likewise, this 'slow burn' also provides time for pneumocyte hyperplasia that prevents direct adhesion of material to the basement membrane. In time, this plug of material may also trap inhaled air and lead to secondary emphysema and/or bronchiectasis.[1,3]. Whether or not left-sided heart failure in conjunction with oxygen therapy (and generation of radical oxygen species) was sufficient to damage the endothelium and/or type I pneumocytes was not resolved in the conference discussion. Herein we use 'fibrinous' and 'organizing' to capture the nature and distribution of this material and introduce this term to a wider audience.

Finally, conference participants touched on the heart failure aspect of this case. Hemosiderin-laden macrophages were a more subtle pickup in this case absent the history, though some participants also noted erythrophagocytosis which was another confirmation of chronic congestion and stasis of pulmonary blood flow. Alveolar macrophages stained strongly with Perl's Prussian blue, confirming the presence of iron.

References:

1. Al-Khouzaie TH, Dawamneh MF, Hazmi AM. Acute fibrinous and organizing pneumonia. *Ann Saudi Med*. 2013 May-Jun;33(3):301-3.
2. Baque-Juston M, Pellegrin A, Leroy S, Marquette CH, Padovani B. Organizing pneumonia: what is it? A conceptual approach and pictorial review. *Diagn Interv Imaging*. 2014 Sep;95(9):771-7.
3. Bharti JN, Satyendra BT, Shekhawat RS, Gorchiya A. Acute Fibrinous and Organizing Pneumonia—A Rare Lung Pathology. *The American Journal of Forensic Medicine and Pathology* 43(1):p e1-e3, March 2022.
4. Caswell JL, Williams KJ. Respiratory System. In: Maxie MG, ed. *Jubb, Kennedy, and Palmer's Pathology of Domestic Animals*. Vol 2. 6th ed. St. Louis, MO: Elsevier; 2016: 485, 489, 493, 509-511, 514, 517, 518, 519.
5. Husain AN. The lung. In: Kumar V, Abbas AK, Fausto N, Aster JC, eds. *Robbins and Cotran Pathologic Basis of Disease*. 10th ed. Philadelphia, PA: Elsevier; 2021:676-678.
6. Kumar V, Abbas AK, Aster JC, eds. *Robbins and Cotran Pathologic Basis of Disease*. 10th ed. Philadelphia, PA: Elsevier; 2021:118.
7. López A, Martinson SA. Respiratory System, Thoracic Cavities, Mediastinum, and Pleurae. In: Zachary JF, ed. *Pathologic Basis of Veterinary Disease*. 7th ed. St. Louis, MO: Elsevier; 2022:571, 574-575, 577-578, 588, 638.
8. Sokol SA, Agnew DW, Lewis AD, Southard TL, Miller AD. Pulmonary hyalinosis in captive sugar gliders (Petaurus breviceps). *J Vet Diagn Invest*. 2017;29(5):691-695.

CASE III:

Signalment:
3.5 year-old, intact female, Drill, *Mandrillus leucophaeus*, non-human primate.

History:
The animal was kept in a zoo with access to indoor- and outdoor facilities. It was presented to the veterinarian due to a mass in the anterior chamber of the left eye. The left eye was removed and submitted for further inves

Figure 3-1. Eye, drill. Inspection of the left eye revealed a yellowish brown, and immovable mass filling the nasoventral part of the left anterior eye chamber (*Photo courtesy of:* Institute of Veterinary Pathology at the Centre for Clinical Veterinary Medicine, Ludwig-Maximilians-Universität München https://www.patho.vetmed.uni-muenchen.de)

tigation to the Institute of Veterinary Pathology at the Ludwig-Maximilians-Universität in Munich, Germany.

Gross Pathology:
In situ-inspection of the left eye revealed a yellowish brown, and immovable mass filling the nasoventral part of the left anterior eye chamber. After removal of the eye and 24 hours of fixation with modified Davidson solution, the mass was further examined and trimmed. The mass measured ca. 1 cm x 0.8 cm x 0.3 cm and was confined to the iris and ciliary body. On cut section, the surface of the iris and ciliary body appeared solid to cystic. The lens was mildly displaced.

Laboratory Results:
Echinococcus multilocularis - PCR (lung, liver, eye): positive.

Echinococcus multilocularis – Immunohistochemistry (eye): positive.

Microscopic Description:
Left eye: The stroma of the iris and ciliary body is focally extensively expanded by a multiloculated hydatid cyst accompanied by marked inflammatory cell infiltration and necrosis. In particular, the iridociliary stroma is partly effaced by multiple intact or collapsed cystic spaces of different sizes (ranging from 15 to 1500 µm in diameter) surrounded by a 10-15 µm thin hyaline acellular laminated cyst wall (laminated layer). The inner part of the cyst wall is often lined by a monolayer of cuboidal cells (germinal layer). The cystic spaces are either optically empty or simply contain finely granular amphophilic material (non-fertile hydatid cyst). The cyst walls are surrounded by numerous multinucleated giant cells with up to 60 nuclei that are irregularly distributed within the cytoplasm (foreign-body giant cells), intermingled with large numbers of macrophages, lymphocytes, and plasma cells, and lower numbers of eosinophilic granulocytes. Intralesionally, there are multiple areas consisting of small cyst wall fragments and cellular debris characterized by loss of cellular detail, hypereosinophilia, and shrinked and fragmented nuclei (necrosis). The expanded iris adheres to the cornea (anterior synechia) and the associated part of the iridocorneal angle is closed.

Moderate to large numbers of plasma cells, lymphocytes, and macrophages are infiltrating the remaining portions of the iridociliary stroma, the trabecular meshwork, as well as the immediately surrounding portions of the choroidea, sclera, and cornea.

Additionally, ocular adnexa including the conjunctiva show multifocal infiltration of

Figure 3-2. Eye, drill. Marked expansion of iris and ciliary body. The mass is partly solid, and partly cystic, displacing adjacent structures including the lens. Scale bar = 1 cm. (*Photo courtesy of:* Institute of Veterinary Pathology at the Centre for Clinical Veterinary Medicine, Ludwig-Maximilians-Universität München https://www.patho.vetmed.uni-muenchen.de)

low to moderate numbers of lymphocytes and plasma cells.

Contributor's Morphologic Diagnosis:
Left eye: Hydatid cyst, multiloculated, non-fertile, iridociliary, with marked chronic granulomatous and eosinophilic anterior uveitis with stromal necrosis, anterior synechia, and mild to moderate chronic lymphoplasmacytic scleritis and conjunctivitis.

Contributor's Comment:
Echinococcus multilocularis (EM) belongs to the phylum *Platyhelminthes*, class *Cestoda* (tapeworms), and subclass *Eucestoda*. Within the order *Cyclophyllidea* it is further subordinated to the family *Taeniidae*. The larval stage of EM is the causative agent of alveolar echinococcosis (AE), a parasitic zoonotic disease of great medical and veterinary importance distributed in the northern hemisphere.[2,8]

The parasite's life cycle usually involves various species of wild rodents, such as *Arvicolinae and Cricetinae*, and the lagomorph pika (*Ochotona curzoniae)* on the Tibetian plateau of China as intermediate hosts. Depending on the epidemiological setting, wild or domestic canid and felid species such as red or arctic foxes, jackals, wolves, dogs, and cats serve as the parasite's definitive hosts.[2,3,7,8] Moreover, dogs can simultaneously act as definitive and intermediate hosts.[2]

The definitive host harbors the egg-producing adult form of EM (tapeworm) within the intestine and eggs or the egg containing last segment of the worm (gravid proglottid) are shed via feces. The infective eggs are dispersed in the environment, where they can survive approximately 1 year in a suitable, moist environment at lower temperatures, but they are sensitive to desiccation and high temperatures.[3] Once the eggs are ingested by the intermediate host, they hatch in the small intestine. The hexacanth larva (oncosphere) is released and penetrates the gut wall. It then passes through the portal and lymphatic vessels, eventually reaching various organs in the intermediate host's body.[8,11] Within the affected organs of the intermediate host, the oncosphere develops into a metacestode, which is a larval stage characterized by multilocular vesiculated cyst formation. This disease is called 'alveolar echinococcosis' due to the appearance of these cysts.[1]

These cysts have an outer laminated layer and an inner germinal layer, and in case of fertile cysts, the germinal layer produces brood capsules containing protoscoleces.[4] The life cycle is completed when the definitive host consumes the organs of the intermediate host that contain fertile metacestodes. Within the intestine, the protoscoleces develop into adults. The prepatent period between ingestion of protoscoleces and the production of eggs by the matured tapeworm

Figure 3-3. Eye, drill. Midline section through globe. There is cystic space-occupying mass within the uvea and choroid at the base of the iris root and ciliary body. (HE, 5X)

typically ranges from 4 to 7 weeks.[8]

Aberrant intermediate host animals and humans can also become infected with the metacestode stage by accidental ingestion of oncosphere-containing eggs.[3] However, aberrant intermediate host animals do not play a role in the transmission cycle and include horses, cattle, domestic and wild pigs, nutria (*Myocastor coypus*), and several species of nonhuman primates (NHP).[3,11] Infection with EM metacestodes is reported from a variety of NHP, including gorilla (*Gorilla gorilla*), orangutan (*Pongo pygmaeus*), rhesus monkey (*Macaca mulatta*), cynomolgus monkey (*Macaca fascicularis*), lion-tailed macaque (*Macaca silenus*),[1,9] Japanese monkeys (*Macaca fuscata*),[5] and ring-tailed lemur (*Lemur catta*).[6] After a large outbreak in a German breeding enclosure with three different affected NHP species, cynomolgus monkeys were considered to be at higher risk, and therefore, presumably are more susceptible to infection than other NHP species. However, it is important to note that NHP in zoological gardens and institutional colonies, particularly in endemic regions, are at risk of becoming infected with EM.[9]

AE is of increasing concern globally due to the geographical spread of EM, its increasing prevalence in animals from endemic areas, the absence of a vaccine, and the lack of active control measures to prevent the infection.[2]

Once the aberrant intermediate host is infected, the metacestode infiltration and proliferation progress silently (in humans, over the course of 5 to 15 years), causing AE, a chronic and complex disease with a devasting clinical condition and high fatality rate if left untreated.[2,8]

AE primarily affects the liver in intermediate hosts as well as aberrant intermediate hosts and behaves like an infiltrative and eventually metastasizing tumor with further infiltration of tissues close to the liver or dissemination via blood and lymphatic vessels.[2,8,11] Less frequently than the liver are lungs, brain, bones, or any other organ of the (aberrant) intermediate host affected.[9,11] Immune suppression exacerbates disease progression.[2,8]

In the present case, a full body necropsy was carried out after the evaluation of the eye, and a subsequent histological examination of further organs failed to identify any additional diseases or evidence of immunosuppression. However, besides the earlier diagnosed intraocular invasion, multiple organs were affected by larval infection, including both common and less common tissues including liver, kidneys, lungs, heart, lymph nodes, skeletal muscles, and brain. The laminated layer of the cysts displayed consistently positive PAS-reactivity. In addition, none of the cysts in this animal contained brood capsules with protoscoleces (non-fertile cysts). In general, fertility of EM cysts is common in susceptible hosts, where it is reached within

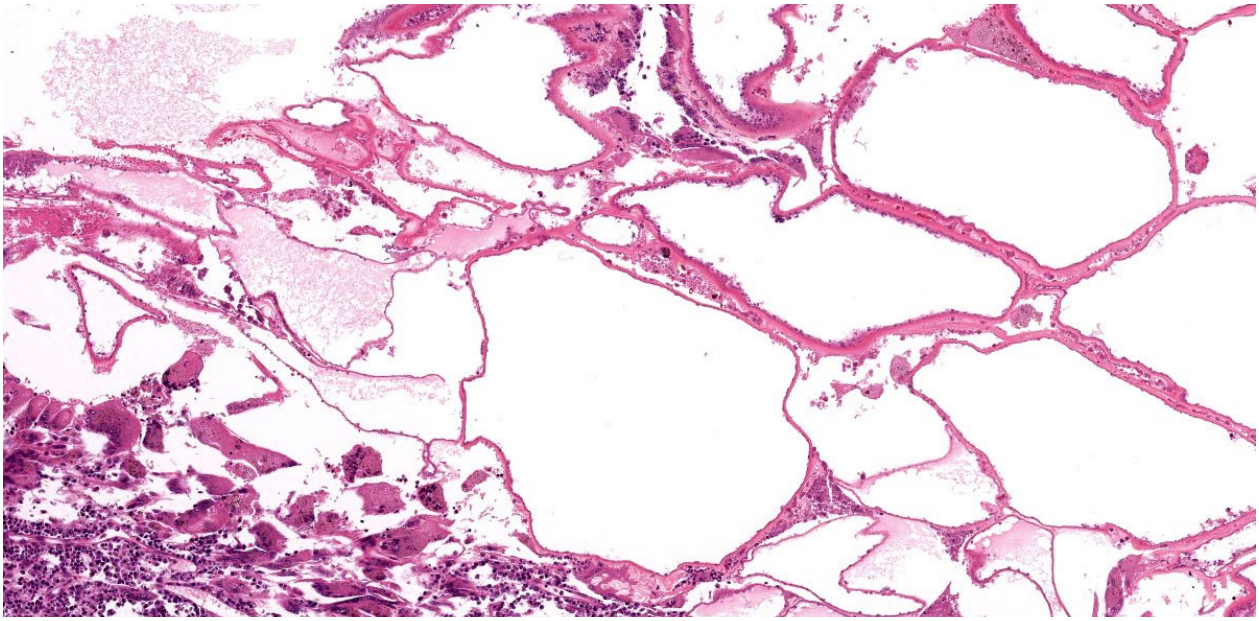

Figure 3-4. Eye, drill. The uveal mass consists of a microcyst of *E. multilocularis* embedded in granulomatous inflammation. The cysts are devoid of protoscoleces, indicating an infertile microcyst. There are numerous multinucleated foreign body-type macrophages at bottom left. (HE, 99X)

2–4 months. But it is far rarer (<20%) in resistant hosts, such as humans, or most domestic animals[8]. Aside from the absent brood capsules and protoscoleces, typical calcareous corpuscles were also not seen in the present case. These corpuscles can be very helpful for identification purposes in histological sections and appear as basophilic to clear ovals with a concentric ringed appearance, but they may "dissolve" in fixation or histological processing.[4]

In human as well as veterinary medicine, the gold standard for AE diagnosis is the identification of parasite structures/genome in samples obtained invasively. Imaging techniques demonstrate characteristic features of the lesions, while serology is complementary.[2,3]

In 2020, an international consensus on terminology to be used in the field of echinococcosis was published. To harmonize echinococcosis terminology on sound scientific and linguistic grounds, the World Association of Echinococcosis launched a Formal Consensus process. The main achievements of this process were: (1) an update of the current nomenclature of *Echinococcus* spp.; (2) an agreement on three names of diseases due to *Echinococcus* spp.: Cystic Echinococcosis, Alveolar Echinococcosis, and Neotropical Echinococcosis, and the exclusion of all other names; (3) an agreement on the restricted use of the adjective "hydatid" to refer to the cyst and fluid due to *E. granulosus sensu lato*; and (4) an agreement on a standardized description of the surgical operations for CE, according to the "Approach, cyst Opening, Resection, and Completeness" (AORC) framework. In addition, 95 "approved" and 60 "rejected" terms were listed.[10] In detail, the term "hydatid" (as noun and as adjective) as well as the term "cyst" should be restricted (by usage, not strictly by definition) to the metacestode of *E. granulosus sensu lato* causing cystic echinococcosis. It should not be used for the metacestode of *E. multilocu-*

laris. This consensus was processed and published in order to avoid confusion between human diseases caused by the various species of *Echinococcus*. "Hydatid" should further not be used to designate anything relating to AE or neotropical echinococcoses caused by *E. vogeli* or *E. oligarthra*. Among all the specialists working in the field of echinococcosis, such as in experimental models, veterinary pathologists are also asked to use the term (echinococcal) "microcyst" in AE lesion instead of the term "hydatid cyst."[10]

Further parasites that can be found incidentally in the animal eye:[12]

- *Echinococcus* in nonhuman primates
- *Cysticercus* in swines
- Microfilariae of *Elaeophora schneideri* in elks causing occlusive vasculitis with multifocal ischemic chorioretinitis and optic neuritis in elks
- fortuitous localization of larvae of *Toxocara canis* or other ascarids, *Angiostrongylus vasorum* and *Dirofilaria immitis* in canine species, associated with uveitis
- Larvae of *Onchocerca cervicalis* and adults of *Setaria* spp. in horses
- Fly larvae in various species causing ophthalmomyasis due to intraocular migration
- Larvae of *Diplostomum spathaceum* in fishes
-

The lens fluke (*Diplostomum spathaceum*) is the only known specific intraocular parasite. This parasite is primarily found in the eye lenses of fishes. After penetrating the fish's skin, the *Diplostomum* larvae migrate to the lens of the eye with remarkable speed and specificity. The presence of numerous larvae within the lens can lead to the development of cataracts. These larvae are ingested by fish-eating birds, which completes the life cycle of the parasite.[12]

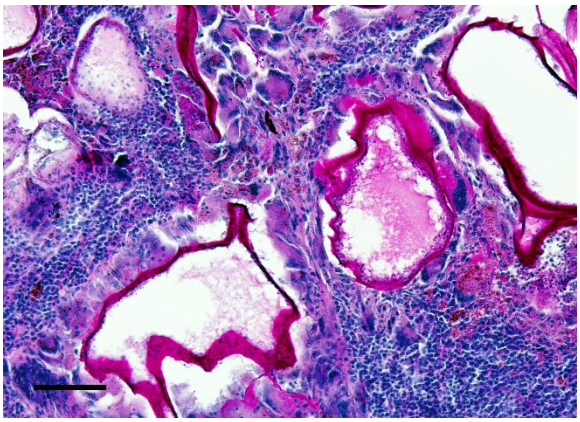

Figure 3-5. Eye, drill. A periodic acid-Schiff stain highlights the hyaline wall of the microcyst. (PAS, 200X) (*Photo courtesy of:* Institute of Veterinary Pathology at the Centre for Clinical Veterinary Medicine, Ludwig-Maximilians-Universität München, https://www.patho.vetmed.uni-muenchen.de)

Contributing Institution:

Institute of Veterinary Pathology at the Centre for Clinical Veterinary Medicine

Ludwig-Maximilians-Universität München
Veterinärstrasse 13

D-80539 Munich, Germany

https://www.patho.vetmed.uni-muenchen.de

JPC Diagnosis:
Eye: Panuveitis, granulomatous, focally extensive, severe, with anterior synechiae, lymphohistiocytic conjunctivitis, and hydatid cyst.

JPC Comment:
The contributor provides a detailed writeup on *Echinococcus* that accompanies great gross photos and an interesting histologic presentation.

Conference participants discussed ancillary changes within the eye which included clo-

sure of the iridocorneal angle and mild corneal edema beyond the other changes the contributor notes. Though there was a mild amount of fibrin lining the contralateral iridocorneal angle, this animal likely did not have sufficient deficit in aqueous humor drainage to cause glaucoma – comparison to the optic nerve, retina, and Descemet's membrane were helpful checks in this case to confirm that histologically. The lack of calcareous corpuscles or protoscoleces in histologic section of this infertile microcyst frustrated some conference participants, though recognition of the thick cyst wall (largely host derived) and germinal lining epithelium were key features. As the contributor hints at, the long duration of this infection in a resistant host makes identifying these features important as they may be the only specific ones that point to *Echinococcus* in these diagnostic cases. For comparison to a more acute infection in a Barbary ape, see VSPO D-P28A for examples of all representative organism features.

This case highlights the potential confusing nomenclature that arises with the shift (and adoption) of new terms to describe entities. Adoption of 'microcyst' and alveolar echinococcosis stymied some of the participants who felt that the morphologic diagnosis should retain the historical term as this change enters veterinary literature and awareness. In solidarity with the contributor, we kept the term hydatid cyst for this conference, but invite readers to explore the reference by Vuitton et al[10] that the contributor helpfully provides.

References:

1. Bacciarini L, Gottstein B, Pagan O, Rehmann P, Gröne A. Hepatic alveolar echinococcosis in cynomolgus monkeys (Macaca fascicularis). *Vet Pathol*. 2004;41:229-234.
2. Casulli A, Barth TFE, Tamarozzi F. Echinococcus multilocularis. *Trends Parasitol*. 2019;35:738-739.
3. Eckert J, Deplazes P. Biological, epidemiological, and clinical aspects of echinococcosis, a zoonosis of increasing concern. *Clin Microbiol Rev*. 2004;17:107-135.
4. Gardiner CH, Poynton SL. Morphological characteristics of cestodes in tissue section. In: *An Atlas of Metazoan Parasites in Animal Tissues*. Washington, DC: Armed Forces Institute of Pathology, American Registry of Pathology; 2006:50-55.
5. Kishimoto M, Yamada K, Yamano K, et al. Significance of imaging features of alveolar echinococcosis in studies on nonhuman primates. *Am J Trop Med Hyg*. 2009;81:540-544.
6. Kondo H, Wada Y, Bando G, Kosuge M, Yagi K, Oku Y. Alveolar hydatidosis in a gorilla and a ring-tailed lemur in Japan. *J Vet Med Sci*. 1996;58:447-449.
7. Oksanen A, Siles-Lucas M, Karamon J, et al. The geographical distribution and prevalence of Echinococcus multilocularis in animals in the European Union and adjacent countries: a systematic review and meta-analysis. *Parasit Vectors*. 2016;9: 519.
8. Tamarozzi F, Brunetti E, Vuitton D. Echinococcosis. In: Fabrizio B, ed. *Helminth Infections and their Impact on Global Public Health*. 2nd ed. Cham: Springer; 2022:257-312.
9. Tappe D, Brehm K, Frosch M, et al. Echinococcus multilocularis infection of several Old World monkey species in a breeding enclosure. *Am J Trop Med Hyg*. 2007;77:504-506.
10. Vuitton DA, McManus DP, Rogan MT, et al. International consensus on terminology to be used in the field of echinococcoses. *Parasite*. 2020;27:41.
11. Wen H, Vuitton L, Tuxun T, et al. Echinococcosis: Advances in the 21st

Century. *Clin Microbiol Rev*. 2019;32.
12. Wilcock BP, Njaa BL. Special Senses. In: Maxie MG, ed. *Jubb, Kennedy & Palmer's Pathology of Domestic Animals.: Volume 1*. 6th ed. St. Louis, Missouri: Elsevier; 2016:407-508.e402.

CASE IV:

Signalment:
11-year-old, female, rhesus macaque, Macaca mulatta, nonhuman primate

History:
This macaque has a history of seven liveborn infants by vaginal delivery and recently delivered a large, liveborn male infant with a body weight of 590 g the day prior to presenting for poor maternal care, a retained placenta and suspected endometritis. On physical examination, the placenta was necrotic with an associated purulent exudate and was manually removed. Samples were submitted for aerobic and anaerobic culture. Supportive and therapeutic care was provided. One week after presentation, the uterus was enlarged on palpation and peritonitis was observed on ultrasound examination. She was referred to surgery for exploratory laparotomy. Peritonitis and multiple uterine ruptures were observed. A hysterectomy was performed.

Figure 4-1. Uterus, rhesus macaque. The uterine body contains three areas of rupture with ragged margins and a fibrinopurulent exudate (*Photo courtesy of:* Oregon National Primate Research Center, https://www.ohsu.edu/onprc)

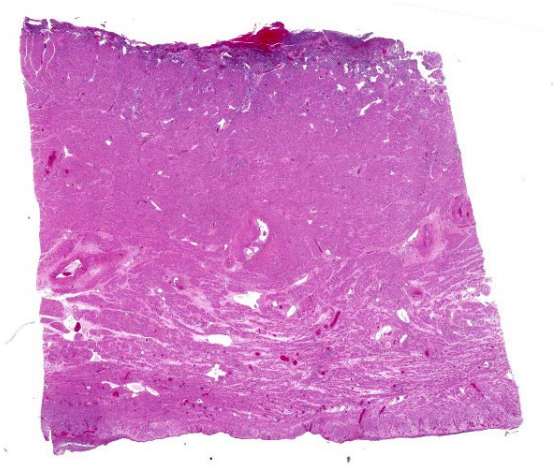

Figure 4-2. Uterus, rhesus macaque. One transmural section of uterus is presented for examination. (HE, 5X)

Gross Pathology:
The uterus is enlarged and the integrity of the uterine fundus and the dorsal aspect of the uterine body is disrupted by three transmural, necrotizing uterine ruptures with ragged margins and a fibrinopurulent exudate.
The placental fragments were not submitted for gross or microscopic examination

Laboratory Results:
Aerobic culture of placental fragments yielded a mixed bacterial population at initial presentation - beta-hemolytic Streptococcus (3+), alpha-hemolytic Streptococcus (not Streptococcus pneumoniae, 2+), Proteus (1+), Staphylococcus aureus (1+), and Staphylococcus epidermidis (1+)
Anaerobic culture of placental fragments at initial presentation yielded gram-positive bacillus (not Listeria, 2+), gram-negative bacillus (2+), and gram-positive coccus (3+)
Cytologic examination of the peritoneal fluid one week following initial presentation

CBC

Reference Intervals	WBC 4,200-13,600	Neuts 2,380-9610	Bands	Lys 1,130-3,770	Monos 190-920	Eos 600-1,100	Bas 20-100	HCT 32.9-41.8	HGB 10.7-13.8	MCV 65.6-76.4	MCHC 31.7 – 33.7	Platelets 119,000-471,000
CBC Results Presentation	7,500	2,400	41%	1,725	225	75	0	34.6	11.3	75	32.8	327,000
CBC Results 12 days later	21,000	13,230	9%	4,620	1,050	210	0	21.6	7.1	74	33	510,000

Serum chemistry

Reference Intervals	TP 6-7.9	ALB 3.3-4.7	ALKP 114-482	ALT 18.9-94.2	AST 18-58	GGT 35-72	TBIL 0-0.4	GLU 45-93	BUN 10-27	CREA 0.6-1.0	K 2.9-4.6	Na 136-153	Cl 102-115	Mg 1.6-2.5	P 4.1-7.8
Result 12 days after presentation	5.3	1.9	171	92	149	17	0.25	56	14.6	0.5	4.7	132	101	1.6	4.7

showed gram-negative bacilli within macrophages and neutrophils.
Aerobic culture of the peritoneal cavity one week after initial presentation yielded Streptococcus, nonhemolytic (4+)
Anaerobic culture of the peritoneal cavity one week after initial presentation yielded gram-positive coccus (3+), gram-negative bacillus (3+) and gram-positive bacillus (1+)

Microscopic Description:
The microarchitecture of the endometrium exhibiting variable stromal decidualization is effaced and overlain by an inflammatory infiltrate composed of myriad degenerate neutrophils, macrophages often laden with brown pigment and fewer lymphocytes admixed with karyorrhectic cellular debris, fibrin, hemorrhage and edema. Endothelial hypertrophy is prominent and there is diffuse congestion. Rare intravascular fibrin thrombi are present. The myofibers of the myometrium immediately subjacent to the endometrium exhibit multifocal, single cell necrosis and multifocally throughout the myometrium there is increased vacuolation of the myofibers. The myometrial interstitium is moderately expanded by fibrous connective tissue and an inflammatory infiltrate composed largely of lymphocytes and plasma cells with few neutrophils surrounds the vasculature. Foci of trophoblastic transformation are present multifocally in the myometrium. The serosa is expanded by degenerate neutrophils, macrophages, fibrin, hemorrhage and karyorrhectic cellular debris. A mixed bacterial population is present within the endometrium and the serosa.

Contributor's Morphologic Diagnosis:
Uterus: Endometritis, necrotizing, fibrinous, exudative, neutrophilic, histiocytic, lymphocytic, chronic-active, diffuse, severe with serositis, rhesus macaque, Macaca mulatta, nonhuman primate.
Myometrium: Vacuolation, myofibers, generally midsection of the uterus, multifocally extensive, moderate with mild perivascular lymphocytic and plasmacytic infiltrates and moderate interstitial fibrosis.
Oviduct (tissue not submitted): Mesosalpingitis, necrotizing, fibrinous, exudative, neutrophilic, histiocytic, lymphocytic, chronic-active, multifocal, moderate.

Contributor's Comment:
Placental retention, an obstetrical complication may occur with uterine atony or with the placenta accreta spectrum characterized by abnormal adherence of the placenta to the placental bed of the uterus.[11] Both entities result in impaired separation and thus release of the placenta. Cervical closure prior to the expulsion of the placenta also results in retained

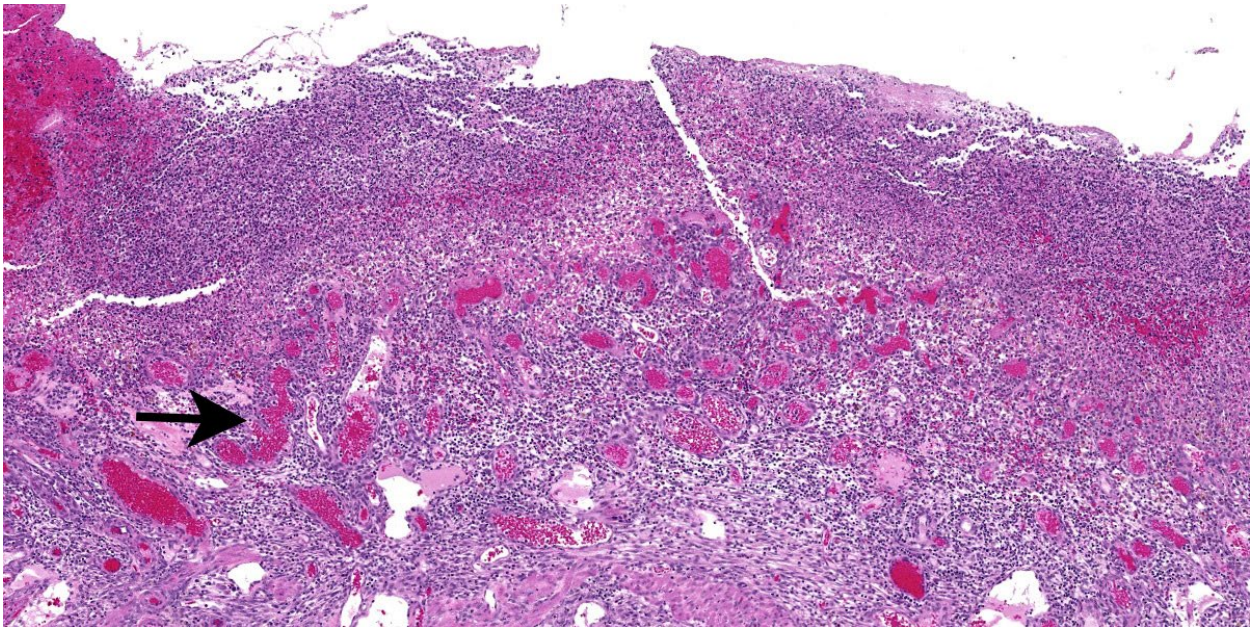

Figure 4-3. Uterus, rhesus macaque. The luminal surface contains decidua infiltrated by large numbers of neutrophils. Spiral arteries may be seen in the deep part of the decidua (arrow). (HE, 5X)

placenta.[11] Clinically, the cervix was open in this case. Placenta accreta, increta or percreta may lead to uterine rupture and were not observed on microscopic examination of the submitted tissues. There was no history of uterine trauma or cesarean section that would increase the risk of uterine rupture. In addition to the chronic-active inflammation, this macaque also had moderate interstitial fibrosis in the myometrium and vacuolation of myofibers which may have hampered effective contractions in expelling the infant and placenta. A retained placenta and uterine rupture with resulting hemorrhage would account for the laboratory findings of a normocytic, normochromic anemia and hypoproteinemia and hypoalbuminemia noted 12 days after clinical presentation. The inflammation present in the uterus and abdominal cavity most likely contributed to the depressed albumin levels as albumin is a negative acute phase reactant and also accounted for the remarkable degenerative left shift of 41% in the leukogram at presentation. The pathogenesis in this case of placental retention, endometritis and multiple uterine ruptures followed by peritonitis was considered to be a prolonged, difficult labor involving a large infant, consequent placental retention due to inadequate myometrial contractions and a subsequent, ascending infection through the vagina and open cervix.[6]

Retained placenta is not an uncommon finding in the breeding colony of rhesus macaques at the Oregon National Primate Research Center. A brief review of the scientific literature revealed a relatively low number of documented cases in nonhuman primates including baboons (*Papio spp.),*[1] cynomolgus macaques (*Macaca fascicularis*),[1,10] rhesus macaques (Macaca mulatta),[1] pigtailed macaques (*Macaca nemestrina*),[12,13] a bonobo (*Pan paniscus*),[7] a golden lion tamarin (*Leontopithecus rosalia*)[4] and a chimpanzee (*Pan troglodytes*).[5] Retained placentas in humans range from 1 – 3% of vaginal deliveries.[11]

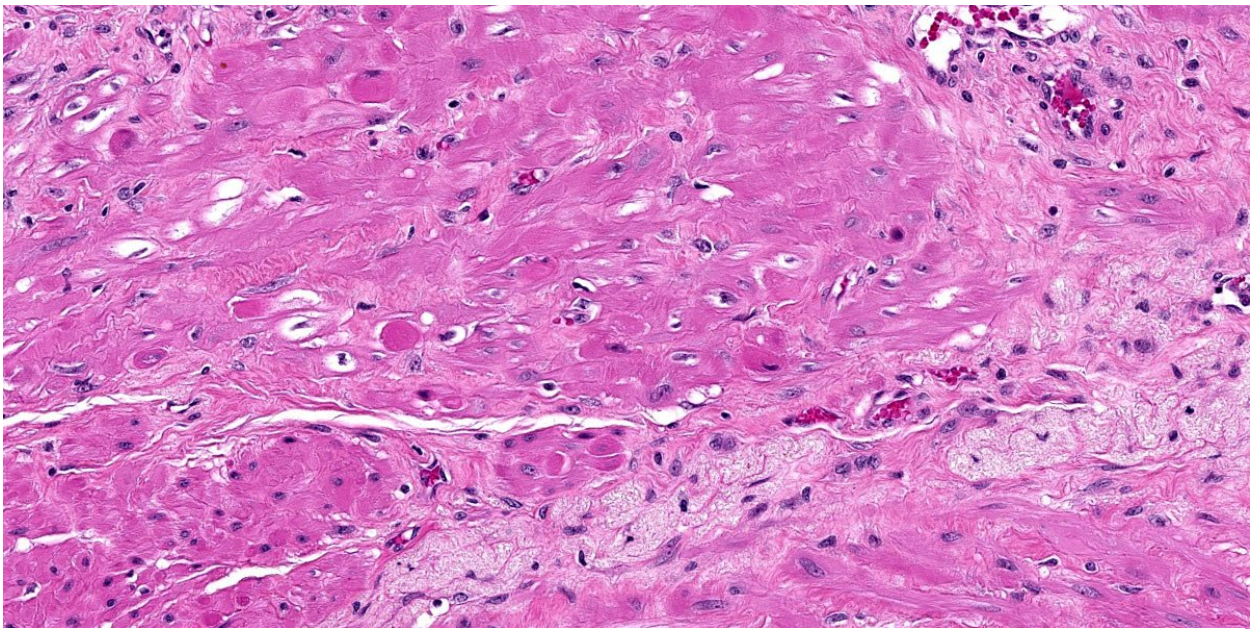

Figure 4-4. Uterus, rhesus macaque. There is scattered degeneration of smooth muscle within the uterine wall. (HE, 259X)

Contributing Institution:
Pathology Services Unit
Division of Animal Resources and Research Support
Oregon National Primate Research Center
505 NW 185th Avenue
Beaverton, OR 97006
https://www.ohsu.edu/onprc

JPC Diagnosis:
Uterus: Endometritis, necrohemorrhagic and suppurative, diffuse, marked with endometrial decidual change, multifocal myometrial degeneration necrosis, and fibrinosuppurative serositis.

JPC Comment:
The final case of this conference provided a challenge as tissue identification was not immediately obvious, though the large amount of irregularly arranged smooth muscle was a helpful feature for recognizing the uterus.

Likewise, participants were not aware of the history of this animal before conference, and considered whether the presence of small-caliber blood vessels and loose endometrial stroma could be evidence of granulation tissue secondary to endometritis. In fact, this was actually retained decidua, representing a transient but important part of the maternal uterine connection to the developing fetus and placenta. Similar to granulation tissue, the decidua is modified endometrium composed of large stromal cells and new blood vessels.[6] The decidua is formed as part of the menstrual cycle and persists with the establishment of pregnancy. Following parturition, the decidua is shed with the placenta, typically within 24 hours.[6] In normal uterine involution, this is represented histologically as regional foci of hemorrhage, inflammatory cells, and necrosis. In this animal however, the placenta was not immediately shed and the degree of inflammation and hemorrhage within the endometrium is entirely in excess. Some participants also noted endometrial spiral arteries in long section which should have also regressed post-partum as another indication of placental retention in this case. Partic

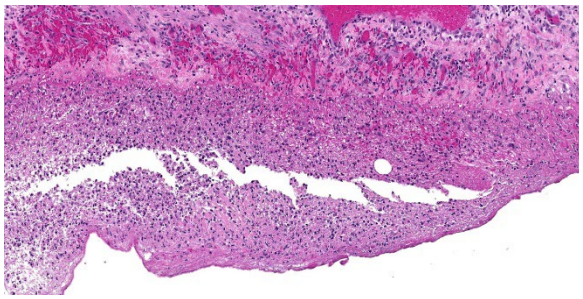

Figure 4-5. Uterus, rhesus macaque. Although the rent in the uterine wall is not evident in the submitted section, there is a fibrinosuppurative exudate expanding the mucosa, and hemorrhagic granulation tissue within the deepest layer of the myometrium above. (HE, 127X)

ipants did not feel confident that they recognized trophoblasts or syncytial trophoblasts amid the large amount of necrotic debris or embedded deeper within the uterine wall, however.

The degree of uterine myometrial degeneration and fibrosis may represent the cause of uterine rupture in this case. The history of difficult delivery in this animal may be correlated to decreased contractility and ability to expel a large fetus, with the resulting increase in uterine pressure from labor stretching this tissue even further and weakening it. Conference participants surmised that seven previous deliveries may have contributed to these myometrial changes, but that the retained placenta *per se* was not the initiating cause. The changes in this case were probably consistent with a placental accreta which is defined by an abnormally strong connection to the endometrium by trophoblasts. In contrast, placental increta represent invasion of trophoblasts into the myometrium with placental percreta extending through the uterus entirely and attaching to other viscera such as the urinary bladder.

Finally, this conference concluded with a discussion of resources for considering placental pathology given the large variation between species and even among non-human primates. We have listed these in the references[2,3,8] as a courtesy for our readers.

References:

1. Bauer C and Harrison T. Retrospective Analysis of the Incidence of Retained Placenta in 3 Large Colonies of NHP. *Comp Med*. 2016; 66(2):143–149.
2. Benirschke, Kurt. Comparative Placentation. UC San Diego. 2012. <http://placentation.ucsd.edu/index.html>.
3. Bowen R. Placental Structure and Classification. Colorado State University. 2011. <https://vivo.colostate.edu/hbooks/pathphys/reprod/placenta/structure.html>.
4. Bronson E, Deem SL, Sanchez C, Murray S. Placental Retention in a Golden Lion Tamarin (Leontopithecus rosalia). J. Zoo Wildl. Med. 2005;36(4):716-718.
5. Calle PP and Stringfellow C. Clinical Challenge: Case 2. *J. Zoo Wildl. Med*. 1991; 22(1):143-145.
6. Cline JM, Brignolo L, Ford EW. Urogenital System/Genital System Female/Placental Disorders. In: Abee CR, Mansfield K, Tardif S, Morris T, eds. *Nonhuman Primates in Biomedical Research: Diseases*. 2nd ed. New York, NY: Elsevier: 2012;522 and 532-533.
7. Halbwax M, Mahamba CR, Ngalula AM, Andre C. Placental retention in a bonobo (Pan paniscus). *J Med Primatol*. 2009;38:171-174.
8. Laurent L, Parast M, Mestan K .Comparative Placentation. UC San Diego. 2024. <https://perinataldiscovery.ucsd.edu/comparative-placentation/species-index/index.html>.
9. Mori M, Bogdan A, Balassa T, Csabai T, Szekeres-Bartho J. The decidua-the maternal bed embracing the embryo-maintains the pregnancy. *Semin Immunopathol*. 2016 Nov;38(6):635-649.
10. Naiken S, Griffiths MA, Edouard L, Pa-

dayatchy N. Factors Influencing Reproduction in Captive-Bred Cynomolgus Monkeys (Macaca fascicularis) From Mauritius. *Am. J. Primatol*. 2015;77:1290–1298.
11. Perlman NC and Carusi DA. Retained placenta after vaginal delivery: risk factors and management. *Int. J. Women's Health*. 2019;11:527-534.
12. Ruch TC. Diseases of the Endocrine, Reproductive and Urinary Systems/Reproductive System. In: Ruch TC ed. *Disease of Laboratory Primates*. Philadelphia, PA: W.B. Saunders Company: 1959;457.
13. Stockinger DE, Torrence AE, Hukkanen RR, Vogel KW, Hotchkiss CE, Ha JC. Risk Factors for Dystocia in Pigtailed Macaques (Macaca nemestrina). *Comp Med*. 2011;61(2):170-175.